NIH Public Access
Author Manuscript
J Biol Chem. Author manuscript; available in PMC 2006 January 25.

Published in final edited form as:
J Biol Chem. 2001 November 9; 276(45): 41733–41741.

Membrane Topography and Topogenesis of Prenylated Rab Acceptor (PRA1)*

Jialing Lin‡, **Zhimin Liang**, **Zhi Zhang**, and **Guangpu Li**‡,§
From the Department of Biochemistry and Molecular Biology, University of Oklahoma Health Sciences Center, Oklahoma City, Oklahoma 73104

Abstract

The mouse prenylated Rab acceptor (mPRA1) is associated with the Golgi membrane at steady state and interacts with Rab proteins. It contains two internal hydrophobic domains (34 residues each) that have enough residues to form four transmembrane (TM) segments. In this study, we have determined the membrane topography of mPRA1 in both intact cells and isolated microsomes. The putative TM segments of mPRA1 were used to substitute for a known TM segment of a model membrane protein to determine whether the mPRA1 segments integrate into the membrane. Furthermore, *N*-linked glycosylation scanning methods were used to distinguish luminal domains from cytoplasmic domains of mPRA1. The data demonstrate that mPRA1 is a polytopic membrane protein containing four TM segments. These TM segments act cooperatively during the translocation and integration at the endoplasmic reticulum membrane. All hydrophilic domains are in the cytoplasm, including the N-terminal domain, the linker domain between the two hydrophobic domains, and the C-terminal domain. As a result, the bulk of mPRA1 is located in the cytoplasm, supporting its postulated role in regulating Rab membrane targeting and intracellular trafficking.

The prenylated Rab acceptor 1 (PRA1)[1] is a 21-kDa protein that has been cloned from mouse, rat, and human cells for its interaction with Rab proteins in the yeast two-hybrid system (1–3). PRA1 is suggested to function as a regulator of Rab membrane association by coordinating with the GDP-dissociation inhibitor (4). Studies on PRA1 biosynthesis have revealed that it is primarily a Golgi membrane protein, suggesting that it may be integrated into the ER membrane before being transported to the Golgi complex (1,4). However, its membrane topography is unknown.

This study examines the membrane topography of mouse PRA1 (mPRA1). The mPRA1 contains two long internal hydrophobic domains (Fig. 1*A*). The first hydrophobic domain (HD1) contains 34 residues, which could contain a signal anchor sequence to target the nascent polypeptide chain to the endoplasmic reticulum (ER) and initiate translocation across the ER membrane. The second hydrophobic domain (HD2) also contains 34 residues, which could contain a stop-transfer sequence to terminate the translocation. These processes would occur

*This work was supported in part by National Institutes of Health Grant R01-GM62964 (to J. L.) and the Oklahoma Center for the Advancement of Science and Technology Grants HR99-058 (to J. L.) and HR01-090 (to G. L.).

‡ To whom correspondence may be addressed: Dept. of Biochemistry and Molecular Biology, University of Oklahoma Health Sciences Center, 940 S. L. Young Blvd., BMSB 853, Oklahoma City, OK 73104. G. L.: Tel.: 405-271-2227 (ext. 1232); Fax: 405-271-3139; E-mail:guangpuli@ouhsc.edu; J.L.: Tel.: 405-271-2227 (ext. 1216); Fax: 405-271-3139; E-mail:jialing-lin@ouhsc.edu..
§Recipient of a CAREER award from the National Science Foundation.

J. Lin and A. E. Johnson, unpublished data.

[1]The abbreviations used are: PRA1, prenylated Rab acceptor 1; mPRA1, mouse PRA1; GDI, GDP dissociation inhibitor; HD, hydrophobic domain; ER, endoplasmic reticulum; TM, transmembrane; PCR, polymerase chain reaction; BHK, baby hamster kidney; SRP, signal recognition particle; Endo H, endoglycosidase H; Endo H_f, a recombinant Endo H from New England BioLabs; KRM, KOAc-washed rough microsomal membrane; PAGE, polyacrylamide gel electrophoresis; MEM, minimal essential medium; NLS, *N*-glycosylation site; nt, nucleotide(s); TAIL, a 140-residue-engineered sequence containing 3 *N*-linked glycosylation sites.

NIH-PA Author Manuscript
NIH-PA Author Manuscript
NIH-PA Author Manuscript

NIH-PA Author Manuscript

NIH-PA Author Manuscript

NIH-PA Author Manuscript

co-translationally at the ER translocon (5), allowing the translocation and integration of mPRA1 into the ER membrane. The protein would then fold and transport to the Golgi complex via the classic exocytic pathway (6).

According to the Kyte-Doolittle (7) hydropathy analysis of the mPRA1 primary sequence (Fig. 1*B*), the mPRA1 may adopt one of several possible membrane topologies. Because HD1 and HD2 contain enough residues to form four transmembrane (TM) segments, one model suggests that the mPRA1 is a polytopic membrane protein with HD1 and HD2 each passing through the membrane twice, placing all hydrophilic domains (the N-terminal, C-terminal, and linker (L) domains) in the cytoplasm (Fig. 1*D*). The assignment of these hydrophilic domains to the cytoplasmic side (*versus* luminal side) is based on the size of the N-terminal domain (78 residues) and the charge distribution adjacent to the TM domains. Thus, a large and stably folded N-terminal domain and domains containing more positively charged residues are likely to be found on the cytoplasmic side of membranes (8–10). In addition to this model, more possibilities arise if one or more of the putative TM segments fail to function as authentic TM segments. This increases uncertainty of predicting mPRA1 membrane topography from its primary sequence.

The current study tests these membrane topography models experimentally. We have employed several *N*-linked glycosylation-scanning strategies to determine if the hydrophilic domains are in the cytoplasm or in the lumen and if each hydrophobic domain functions as one or two TM segments. These experiments have been conducted in both intact cells (*in vivo* system) and isolated microsomes (*in vitro* system) to ascertain the conclusions. The data show that mPRA1 contains four TM segments and adopts a membrane topography as predicted in Fig. 1*D*. All hydrophilic domains are located in the cytoplasm, suggesting that mPRA1 functions at the cytoplasmic surface of the membrane, consistent with its proposed role in regulating the Rab cycle and intracellular trafficking.

EXPERIMENTAL PROCEDURES

Plasmids

The mPRA1 cDNA (1) was previously cloned at the *Bam*HI restriction site of the plasmid pGEM3 (Promega) in an orientation that its transcription was under the control of a SP6 promoter. This pGEM3/mPRA1 construct was used as a template to generate the mutant constructs pGEM3/mPRA1:G15N, pGEM3/mPRA1:G61S, and pGEM3/mPRA1:L115N by using the QuikChange site-directed mutagenesis method (Stratagene). Each mutant contained an *N*-linked glycosylation site in a different domain of the mPRA1 sequence. To add an *N*-glycosylation site (NLS) to the C terminus of mPRA1, a PCR strategy was employed. The 5′-primer contained a *Bam*HI restriction site, followed by an 18-nucleotide sequence coding for the N terminus of mPRA1, including the ATG codon. The 3′-primer contained a *Bam*HI restriction site, followed by TTA (complementary to TAA termination codon), a 9-nt sequence coding for NLS and an 18-nt sequence complementary to the coding sequence for the C terminus of mPRA1. The PCR product (*i.e.* the mPRA1-NLS cDNA) was digested with *Bam*HI, purified, and ligated back into the *Bam*HI site of pGEM3. All mutations and the entire mPRA1 cDNA sequence were confirmed by using an automatic DNA sequencer (ABI377) (DNA sequencing facility, University of Oklahoma Health Sciences Center). These pGEM3 constructs were used for *in vitro* transcription and translation of mPRA1 and the mutants (see below for details). For expression of these proteins in cultured BHK cells, the cDNAs of mPRA1 and the mutants were excised from the pGEM3 constructs via *Bam*HI digestion, and subcloned into the *Bam*HI site of the mammalian cell expression vector pcDNA3.1 (Invitrogen) under the control of a cytomegalovirus promoter.

NIH-PA Author Manuscript

NIH-PA Author Manuscript

NIH-PA Author Manuscript

C-terminal truncation mutants (mPRA165, mPRA150, mPRA112, and mPRA95) were generated by PCR using the pGEM3/mPRA1 construct as a template. The 5′-primer contained an *Nco*I site and the 3′-primer contained a *Bam*HI site. The PCR products were digested with *Nco*I and *Bam*HI, purified, and ligated into the vector pSPUTK (a generous gift from Dr. David Andrews of McMaster University) (11), which was digested by both *Nco*I and *Bam*HI. The resulting constructs pSPUTK/mPRA165, pSPUTK/mPRA150, pSPUTK/mPRA112, pSPUTK/mPRA95, and pSPUTK/mPRA1 (the wild-type) were then linearized by *Bam*HI digestion and used as vectors for the insertion of the TAIL domain cDNA, which was generated by PCR of pJL111 (12) and digested with *Bam*HI. These pSPUTK constructs were used for *in vitro* transcription and translation of the chimeric proteins, including mPRA165-TAIL, mPRA150-TAIL, mPRA112-TAIL, mPRA95-TAIL, and mPRA1-TAIL. To express these proteins in cultured BHK cells, their cDNAs were subcloned into the pcDNA3.1 vector.

The mPRA(TM1-TAIL*-TM2) and mPRA(TM3-TAIL*-TM4) chimeras were generated by inserting the N-terminal 52 residues of the TAIL domain (TAIL*) between TM1 and TM2 (between residues 93 and 94) or between TM3 and TM4 (between residues 148 and 149) of mPRA1. This was done by using PCR-mediated gene fusion procedure with mPRA1 and TAIL cDNAs as templates. The PCR products were confirmed by DNA sequencing after cloned into pSPUTK or pcDNA3.1.

To make the constructs for the chimeric proteins 111p-TM1, 111p-TM2, 111p-TM3, 111p-TM4, 111p-HD1, and 111p-HD2, the pJL111 plasmid (12) was digested with *Sst*I and *Spe*I to delete the coding sequence for the TM segment of the model protein 111p, and used as a vector for the insertion of the cDNA for the TM1, TM2, TM3, TM4, HD1, or HD2 segment of mPRA1. The cDNAs coding for the mPRA1 TM and HD sequences were generated by PCR of pGEM3/mPRA1 with the corresponding oligonucleotide primers and digested with *Sst*I and *Spe*I prior to the ligations. The resulting constructs were used as templates for *in vitro* transcription and translation to produce the chimeric proteins 111p-TM1, 111p-TM2, 111p-TM3, 111p-TM4, 111p-HD1, and 111p-HD2.

In Vitro Transcription

The above plasmids were linearized with restriction endonucleases downstream the coding region and transcribed *in vitro* using SP6 RNA polymerase as described previously (13), except that 0.3 mM GTP, 0.5 mM diguanosine triphosphate (Sigma), and 0.5 unit/μl RNaseout RNase inhibitor (Life Sciences) were included in the reactions. After 90 min of incubation, [GTP] was brought to 3 mM for an additional 30 min of incubation.

In Vitro Translation

Wheat germ extract was prepared as described previously (14). KOAc-washed rough microsomal membrane (KRM) and SRP were prepared from dog pancreas as described previously (15). Translations using wheat germ extract contained (per 25 μl) 4 μl of the extract, 2 μl of mRNA, 25 mM Hepes, pH 7.5, 90 mM KOAc, pH 7.5, 3 mM $Mg(OAc)_2$, 2 mM glutathione, 0.625 μg of Nikkol, 0.2 mM spermidine, 8 μM *S*-adenosyl-L-methione, 5 μCi of [^{35}S]methionine, 5 units of RNase-out RNase inhibitor, a protease inhibitor mix containing 5 ng of each pepstatin A, chymostatin, antipain, and leupeptin, and 7.5 ng of aprotinin, and an energy-generating system containing 30 mM of each amino acid except methionine, 1.2 mM ATP, 1.2 mM GTP, 9.6 mM phosphocreatine, and 1.92 μg of creatine phosphokinase (Sigma Chemical Co.), and where indicated, 4 equivalents of KRM or 40 nM SRP. Equivalent of KRM was defined previously (15). Translation reactions were conducted at 26 °C for 50 min.

Translations using rabbit reticulocyte lysate (MBI Fermentas) contained (per 25 μl) 12.5 μl of the lysate, 110 mM KOAc, pH 7.5, 1 mM $Mg(OAc)_2$, 50 μM hemin hydrochloride, and other

NIH-PA Author Manuscript

NIH-PA Author Manuscript

NIH-PA Author Manuscript

components as described above for translation with wheat germ extracts, excluding the wheat germ extract and SRP. Translation reactions were conducted at 26 °C for 50 min.

Membrane Topology Analysis

The translation products (10 μl) were: (i) precipitated immediately with the acid Cl_3CCOOH; (ii) denatured in 0.5% SDS, 1% β-mercaptoethanol, and then treated with Endo H_f according to the manufacturer's instructions (New England BioLabs; 80 units/μl, 37 °C, overnight) before the acid precipitation; (iii) diluted with Na_2CO_3 to achieve a final volume of 100 μl and a final concentration of 0.1 M Na_2CO_3 at pH 11.5. The samples were then kept on ice for 10 min before layered onto a 100 μl cushion (0.2 M sucrose, 100 mM Na_2CO_3 at pH 11.5) and centrifuged in a Beckman Optima MAX Ultracentrifuge (TLA-100 rotor, 57,000 rpm, 11 min, 4 °C). The supernatants were divided into two aliquots, top (*T*) and bottom (*B*) fractions, before the acid precipitation. The pellets (*P*) were subjected to SDS-PAGE analysis directly; or (iv) digested with proteinase K (Sigma, 0.25 μg/μl, 22 °C, 1 h) in the absence or presence of 1% Triton X-100 before being quenched with 10 mM phenylmethylsulfonyl fluoride and precipitated with Cl_3CCOOH. All the protein pellets were solubilized in 25 μl of 4% SDS, 17% glycerol, 4% β-mercaptoethanol, 8.6 mM EDTA, 137 mM Tris, pH 9, at 65 °C for 30 min. SDS-PAGE analysis of the samples was done using a 14% or a 10–15% acrylamide gel as indicated in figure legends. The radioactivity in dried gels was quantified by using a PhosphorImager (Molecular Dynamics).

Insoluble precipitants were formed when the translation products from the rabbit reticulocyte lysate system were denatured before the Endo H_f treatment. To avoid this problem, the translation products (10 μl) were diluted with 110 mM KOAc, 1 mM $MgCl_2$, 25 mM Hepes, pH 7.5, to a final volume of 50 μl and then layered onto a 100-μl cushion (0.5 M sucrose, 100 mM KOAc, 5 mM $MgCl_2$, 25 mM Hepes, pH 7.5). After centrifugation in a Beckman Optima MAX Ultracentrifuge (TLA-100 rotor, 50,000 rpm, 4 min, 4 °C), the membrane-bound proteins in the pellet were then denatured and treated with Endo H_f as described above.

Expression of mPRA1 and Its Mutants in Cultured BHK Cells

The pcDNA3.1 constructs containing the cDNAs for mPRA1, its mutants, and chimeras (see above) were transfected into BHK cell monolayers via the LipofectAMINE-mediated procedure (Invitrogen). The BHK cells were grown in 35-mm culture dishes in α-MEM containing 5% fetal bovine serum (Invitrogen). Cells were incubated in a 37 °C incubator with 5% CO_2. At 24-h post-transfection, expression of the desired proteins was examined by either metabolic pulse-chase labeling with [^{35}S]methionine and immunoprecipitation, or immunoblot analysis with the goat antiserum specific for mPRA1.

Pulse-chase Labeling of BHK Cells with [^{35}S]Methionine and Immunoprecipitation

Cells were starved in methionine-free α-MEM for 30 min at 37 °C, followed by a 5-min pulse labeling in the same medium containing [^{35}S]methionine (Tran^{35}S-label from ICN used at 50 μCi/ml) and then chased in normal α-MEM containing 5% fetal bovine serum for either 0 or 30 min. Cells were then lysed in 1% SDS (200 μl per dish), and the lysates were immunoprecipitated (16) with the goat antiserum specific for mPRA1. The immunoprecipitated proteins were analyzed by SDS-PAGE (12% gel), followed by fluorography (treatment with 1 M sodium salicylate for 30 min) and autoradiography (exposure of the dried gel to a Kodak XAR-5 film for 24 h and then development of the film).

Immunoblot Analysis

Cells were lysed in 1% SDS (200 μl per dish), and a half of the lysate was treated with Endo H_f (New England BioLabs) for 4 h at 37 °C. Both Endo H_f-treated and untreated lysates (10

NIH-PA Author Manuscript

NIH-PA Author Manuscript

NIH-PA Author Manuscript

μl each) were analyzed by SDS-PAGE (12% gel), followed by immunoblot analysis using the goat antiserum specific for mPRA1 and the ECL reagents (Amersham Pharmacia Biotech). The antigenic sites apparently included the N-terminal domain of mPRA1, because the antiserum recognized all C-terminal truncation mutants.

Triton X-114 Partitioning Experiment

BHK cell monolayers (about 80% confluent in 35-mm dishes) were transfected with pcDNA3.1/mPRA1 as described above and incubated at 37 °C (5% CO_2) for 24 h. Cells were lysed directly in 200 μl of 10 mM Tris-HCl, pH 7.4, 150 mM NaCl, 1% Triton X-114 at 0 °C. The lysates were partitioned into detergent and aqueous phases according to Bordier's method (17). Triton X-114 and buffer were added to the aqueous and detergent phases, respectively, to obtain identical volume and chemical content for the proteins in the two phases. Proteins in both phases were analyzed by SDS-PAGE (12% gel), and mPRA1 was identified by immunoblot analysis using the goat antiserum monospecific for mPRA1 and the ECL reagents (Amersham Pharmacia Biotech).

Isolation of Membranes from BHK Cells and Na_2CO_3 Extraction

The membrane fractions of BHK cells expressing the mPRA-TAIL chimeric proteins were isolated as described previously (1). The membranes were then resuspended in 100 μl of 0.1 M Na_2CO_3 at pH 11.5 and fractionated as described above under "Membrane Topology Analysis" (iii).

RESULTS

The Membrane Association of mPRA1

The recently cloned mPRA1 (1) was used in this study. Hydropathy analysis of its primary sequence revealed an N-terminal hydrophilic domain (78 residues) (*N*), followed by a hydrophobic domain of 34 residues (*HD1*), a hydrophilic linker domain of 19 residues (*L*), a second hydrophobic domain of 34 residues (*HD2*), and a C-terminal hydrophilic domain of 20 residues (*C*) (Fig. 1, *A* and *B*). Previous subcellular fractionation and fluorescence microscopy experiments indicated that mPRA1 is a membrane protein associated with the Golgi complex (1,4). To confirm this result, we conducted Triton X-114 partitioning experiments in which membrane proteins should partition into the detergent phase. BHK cells expressing mPRA1 were lysed in 1% Triton X-114, and the lysates were allowed to separate into detergent and aqueous phases. Proteins in both phases were analyzed by SDS-PAGE, and mPRA1 was identified by immunoblot analysis. The mPRA1 was found exclusively in the detergent phase (Fig. 1*C*), consistent with the notion that it is an integral membrane protein.

In general, spanning the hydrophobic core of the phospholipid bilayer would require 20 or less hydrophobic amino acids (α-helix or β-sheet). The length of HD1 and HD2 suggested that each could potentially form two TM segments. Taking into consideration the large size of the N-terminal hydrophilic domain and the charge distribution adjacent to the putative TM segments, a membrane topology model was proposed for mPRA1 (Fig. 1*D*).

Identification of TM Segments in mPRA1

To determine if the predicted TM segments in mPRA1 (Fig. 1*D*) indeed function as authentic TM segments, we substituted each of the putative mPRA1 TM segments (TM1–4) for the TM segment of a model membrane protein, 111p (18). The 111p protein has a cleavable signal sequence at the N terminus and a TM segment in the middle that is followed by a "tail" sequence containing three consensus *N*-linked glycosylation sites (Fig. 2*A*). As previously determined (18), 111p integrates into the microsomal membrane in an N-luminal/C-cytosolic (type I)

NIH-PA Author Manuscript

NIH-PA Author Manuscript

NIH-PA Author Manuscript

orientation with its TM segment spanning the lipid bilayer. Because the C-terminal tail sequence, including the glycosylation sites, remains on the cytoplasmic side of the membrane, 111p is not glycosylated.

When the TM segment of 111p was replaced by the TM1 segment (residues 79–94) of mPRA1, the resulting chimeric protein 111p-TM1 was shown to maintain the type I topography upon integration into the microsomal membrane (Fig. 2*B*). The major translation product in the presence of microsomes had signal sequence cleaved, because it was smaller than the product translated in the absence of microsomes (Fig. 2*B*, *lanes 1* and *2*, *arrow*). This major signal sequence-cleaved product was not glycosylated because it was insensitive to Endo H treatment (Fig. 2*B*, *lane 3*). This product was integrated into the lipid bilayer as demonstrated by its insolubility in the sodium carbonate buffer (pH 11.5) (Fig. 2*B*, *lanes 4–6*). Furthermore, this product was partially accessible to proteinase K that was added to the cytoplasmic side, indicating that a part of the protein was exposed at the cytoplasmic side of the membrane (Fig. 2*B*, compare *lanes 7–9*). Taken together, the data indicated that 111p-TM1 adopted the same membrane topography as its parent 111p. Thus, the TM1 segment of mPRA1 functioned as a TM sequence in the model membrane protein. We noticed that a rather minor fraction of the products translated in the presence of microsomes was glycosylated (Fig. 2*B*, *lane 2*, *arrowhead*), which was sensitive to Endo H treatment (Fig. 2*B*, *lane 3*) and was insoluble in sodium carbonate buffer (Fig. 2*B*, *lane 4*). This minor product evidently had the opposite orientation (compared to the major product), which was likely an experimental aberration of the *in vitro* system.

Similar results were obtained for 111p-TM2 and 111p-TM4, indicating that both TM2 (residues 95–112) and TM4 (residues 149–165) were able to maintain the membrane topology of 111p when substituting for its TM segment (Fig. 2, *C* and *D*). Thus, like TM1, both TM2 and TM4 were authentic TM segments in the model membrane protein. In contrast, the TM3 segment (residues 132–148) of mPRA1 failed to function as a TM segment in the model protein (Fig. 2*E*). In this case, the 111p-TM3 product was mostly glycosylated when translated in the presence of microsomes and was consequently larger than the product translated in the absence of microsomes (Fig. 2*E*, *lanes 1* and *2*, *arrowhead*). The glycosylated form was sensitive to Endo H treatment, which resulted in a product smaller than the translation product in the absence of microsomes (Fig. 2*E*, compare *lanes 1*, *2*, and *3*). The data indicated that the 111p-TM3 product synthesized in the presence of microsomes was both signal sequence-cleaved and glycosylated. Furthermore, the glycosylated 111p-TM3 was completely protected from proteinase K digestion by the microsomal membrane (Fig. 2*E*, *lanes 7* and *8*) but could be solubilized by the sodium carbonate buffer (pH 11.5) (Fig. 2*E*, *lanes 4–6*), indicating that the protein was completely in the lumen of the microsomes.

Identification of Functional Pairs of TM Segments in mPRA1

It was reported before that certain TM segments only function when paired with another downstream TM segment (19–21). To determine if TM1 and TM2 or TM3 and TM4 together would function as functional pairs of TM segments, we substituted the entire HD1 (TM1 plus TM2) or HD2 (TM3 plus TM4) for the TM segment of 111p, resulting in the chimeras 111p-HD1 and 111p-HD2, respectively. When 111p-HD1 was translated in the presence of the membranes, 30% of the protein was glycosylated (Fig. 3*A*, *lane 2*, *arrowhead*). This glycosylation efficiency appeared to be the upper limit of the *in vitro* translation system, because a control protein derived from the 111p that had an additional TM segment (from bovine opsin) inserted behind the original TM segment was only 30% glycosylated.[2] The glycosylated form of 111p-HD1 was sensitive to Endo H treatment (Fig. 3*A*, *lane 3*) but resistant to sodium carbonate extraction (Fig. 3*A*, *lanes 4–6*) and completely protected by microsomal membrane from proteinase K digestion (Fig. 3*A*, *lane 7*). These data demonstrated

NIH-PA Author Manuscript

NIH-PA Author Manuscript

NIH-PA Author Manuscript

that the 111p-HD1 was integrated into the membrane with both N- and C-terminal domains in the lumen and HD1 sequence in the lipid bilayer as a pair of TM segments. Taken together with the data on 111p-TM1 and 111p-TM2, we showed here that the HD1 sequence contained two functional TM segments (TM1 and TM2).

Glycosylation was also observed in 111p-HD2, although it was less efficient (about 20%), and there were two distinct glycosylated products (Fig. 3*B*, *lane 2*, *open* and *closed circles*). The glycosylated form I (Fig. 3*B*, *lane 2*, *open circle*) of 111p-HD2 had similar properties as those of glycosylated 111p-HD1, including its sensitivity to Endo H and resistance to Na_2CO_3 extraction and proteinase K digestion (Fig. 3*B*, *lanes 3–8*). These data suggested that HD2 also functioned as two TM segments (TM3 and TM4), although TM3 by itself was unable to function as a TM segment (Fig. 2*E*). We noticed that the glycosylated form I of 111p-HD2 was not as tightly associated with the membrane as 111p-HD1, judging from its partial solubility (about 30%) in the carbonate buffer. Thus, some proteins in this fraction of 111p-HD2 appeared unable to integrate into the lipid bilayer.

The relative low efficiency of glycosylation could be explained if one TM segment in the respective HD sequence sometimes failed to function *in vitro*, leaving only one functional TM segment in each HD sequence. For 111p-HD2, another glycosylated product (the form II; see Fig. 3*B*, *closed circle*) was observed in addition to the glycosylated form I mentioned above. This protein was resistant to Na_2CO_3 extraction but was digested by proteinase K even in the intact microsome, suggesting that this fraction of 111p-HD2 adopted an N-cytosol/C-lumen (type II) topography. This could be explained if the N-terminal signal sequence of this fraction of 111p-HD2 did not function properly. Instead, HD2 served as an internal signal-anchor sequence to translocate the TAIL sequence into the lumen. The formation of these products was likely due to the inefficiency of the *in vitro* system as well as the loss of native context of these TM segments. To clarify this issue, we examined in the following experiments the topogenic function of the TM segments in mPRA1.

Topogenic Function of the Putative TM Segments in mPRA1

To determine how these TM segments would function during integration of mPRA1 into the membrane, the mPRA1 sequence was truncated at residue 95, 112, 150, and 165, respectively, and fused to the “tail” sequence of 111p that contains the glycosylation sites. The resulting chimeric proteins had the reporter “tail” sequence positioned right after each of the putative TM segments of mPRA1 (Fig. 4*A*). These proteins were then synthesized in wheat germ extracts in the absence or presence of microsomes. It was clear that, in the presence of microsomes, mPRA95-TAIL contained a higher molecular weight form (Fig. 4*B*, *lane 2*, *arrowhead*) that was sensitive to Endo H treatment (Fig. 4*B*, *lane 3*), indicating that the TAIL sequence was glycosylated and hence located in the microsomal lumen. Glycosylation of the TAIL sequence was dependent on the addition of signal recognition particle (SRP) to the *in vitro* translation system (Fig. 4*B*, compare *lanes 11* and *12*), indicating that the targeting of mPRA95-TAIL to the microsome utilized the classic SRP-dependent pathway (5). Because the TM1 segment was the only hydrophobic sequence in mPRA95-TAIL, it must have functioned as an internal signal sequence to translocate the downstream TAIL sequence into the microsomal lumen, resulting in an N-cytoplasmic/C-luminal (type II) topography (Fig. 4*B*). In agreement with this contention, proteinase K digestion of the mPRA95-TAIL protein translated in the presence of microsomes generated a proteolytic fragment that was protected by the membrane from further proteinase K digestion (Fig. 4*B*, *lane 8*, *downward arrow*). In addition, this fragment was sensitive to Endo H treatment (Fig. 4*B*, *lane 9*, *upward arrow*), indicating that this protected fragment contained the glycosylated TAIL sequence. Although the glycosylation was inefficient (~10%) in the *in vitro* system, mPRA95-TAIL became 100% glycosylated *in vivo* when it was expressed in BHK cells (Fig. 4F, *mPRA95-TAIL*), supporting

NIH-PA Author Manuscript

NIH-PA Author Manuscript

NIH-PA Author Manuscript

the topological interpretation of the *in vitro* data (Fig. 4*B*). Likewise, although the glycosylated form of *in vitro* translated mPRA95-TAIL was soluble in carbonate buffer (Fig. 4*B*, *lanes 4–6*), it became completely insoluble and thus 100% integrated into the membrane in BHK cells (Fig. 4*G*), confirming that TM1 functioned as both signal-anchor and TM sequence. Nonetheless, the relatively inefficient *in vitro* system allowed us to separate the translocation and integration processes. Thus, the *in vitro* data on mPRA95-TAIL suggested that, although the TM1 segment was able to translocate the TAIL domain into the lumen of microsome, it was incapable of integrating into the bilayer as indicated by its solubility in the carbonate buffer, possibly due to retention by the translocon (12). However, TM1 and TM2 segments together, as in the case of mPRA112-TAIL, were able to effectively integrate into the bilayer *in vitro* (Fig. 4*C*, *lanes 4–6*; see below). This type of cooperativity of a pair of TM segments during an integration event was previously observed with other polytopic membrane proteins (19–21).

The mPRA112-TAIL protein, which had the TAIL sequence fused after the TM2 segment, was not glycosylated when translated in the presence of microsomes (Fig. 4*C*, *lanes 2* and *3*). This indicated that the TAIL sequence was on the cytoplasmic side of microsomal membranes. Because mPRA112-TAIL contained both TM1 and TM2, it was likely integrated into the membrane with both N- and C-terminal domains on the cytoplasmic side, and the TM1 and TM2 segments in the bilayer as shown by the graphic in Fig. 4*C*. This interpretation was consistent with the data on the 111p chimeras (Figs. 2*B*, 2*C*, and 3*A*) and was supported by the following observations. First, some mPRA112-TAIL proteins were insoluble in the sodium carbonate buffer, indicating that they were integrated into the bilayer (Fig. 4*C*, *lanes 4–6*). Although the insoluble fraction was ~50% *in vitro*, it increased to essentially 100% *in vivo* in BHK cells (data not shown but similar to Fig. 4*G*). Second, a large portion of the protein was digested by proteinase K added to the cytoplasmic side, suggesting that the bulk of the protein was located on the cytoplasmic side (Fig. 4*C*, *lane 8*).

The mPRA150-TAIL and mPRA165-TAIL proteins, like mPRA112-TAIL, were not glycosylated when translated in the presence of microsomes (Fig. 4, *D* and *E*), whereas they were effectively integrated into the bilayer (Fig. 4, *D* and *E*, *lanes 4–6*). They were also sensitive to proteinase K digestion (Fig. 4, *D* and *E*, *lanes 7–9*). This was expected for mPRA150-TAIL that contained TM3 in addition to TM1 and TM2, because TM3 alone was not a functional TM segment as determined by using the 111p-TM3 construct (Fig. 2*E*). The fact that mPRA165-TAIL, which contained the entire HD2 (TM3 and TM4) upstream the TAIL domain, was also not glycosylated, suggested that HD2 contained two TM segments. This interpretation would be consistent with the data for 111p-HD2, which showed the existence of two TM segments within the HD2 sequence (Fig. 3*B*).

The relative inefficiency of the *in vitro* translocation/integration assay prompted us to determine the membrane translocation/integration of the mPRA-TAIL chimeras *in vivo*. The mPRA-TAIL chimeric proteins were expressed in BHK cells. Cell lysates were either treated or not treated with Endo H (Fig. 4*F*) or Endo F (data not shown), followed by immunoblot analysis of proteins with the goat antiserum monospecific for mPRA1. Although mPRA-TAIL, mPRA165-TAIL, mPRA150-TAIL, and mPRA112-TAIL were not glycosylated (Fig. 4*F*, *lanes 3–8*), mPRA95-TAIL was completely glycosylated *in vivo* as evidenced by the mobility shift after the Endo H treatment (Fig. 4*F*, *lanes 9* and *10*). Furthermore, we found that the mPRA95-TAIL protein was essentially 100% insoluble in carbonate buffer just like the full-length mPRA-TAIL fusion protein (Fig. 4*G*) and other truncated mPRA-TAIL fusion proteins (data not shown), indicating that they all fully integrated into the membrane *in vivo*. These data confirmed the *in vitro* results and highlighted the much more efficient membrane translocation/integration process *in vivo*. We noticed that the mPRA150-TAIL was not glycosylated even *in vivo*. Therefore, the *in vitro* result that TM3 by itself was unable to translocate the

NIH-PA Author Manuscript

NIH-PA Author Manuscript

NIH-PA Author Manuscript

downstream TAIL sequence across the membrane was not due to the inefficiency of the *in vitro* system but the intrinsic inability of TM3 sequence to serve as a signal sequence.

The mPRA1 Topography

We next addressed the native topography of mPRA1 by introducing *N*-linked glycosylation sites (Asn-*X*-Ser/Thr) in different domains of the native mPRA1 that lack endogenous glycosylation sites and determining whether these sites are utilized for glycosylation (Fig. 5). The mPRA1: G15N and mPRA1:G61S mutants each contained a glycosylation site in the N domain. The mPRA1:L115N mutant contained a glycosylation site in the L domain. The mPRA1-NLS mutant had a glycosylation site added to the C terminus of mPRA1. To test whether these mPRA1 mutants could be glycosylated *in vitro*, these mutants along with the wild-type mPRA1 were translated in rabbit reticulocyte lysates in the absence and presence of microsomes. The mPRA1 and the mutant proteins that were translated in the presence of microsomes were mostly insoluble in the sodium carbonate buffer (pH 11.5) (Fig. 5*B*, *lanes 8–10*; Fig. 5*C*, *lanes 1–3*; data not shown). In contrast, the same proteins that were translated in the absence of microsomes were completely soluble in the same buffer (Fig. 5*B*, *lanes 2–4*; data not shown). The results indicated that these mPRA1 mutants integrated into the microsomal membranes like the wild-type mPRA1. However, none of these mutants was glycosylated based on the following observations. First, the size of the proteins synthesized in the presence of microsomes was indistinguishable from that synthesized in the absence of microsomes (Fig. 5*C*, *lanes 4* and *5*; Fig. 5, *D–F*, *lanes 1* and *2*). Second, the proteins were insensitive to Endo H treatment (Fig. 5*C*, compare *lanes 8* and *9*; data not shown). These *in vitro* data suggested that the N, L, and C domains of mPRA1 were all located in the cytoplasmic side of the membrane. Several higher molecular weight proteins were produced when translations were conducted in the presence of microsomes (Fig. 5*C*, compare *lanes 4* and *5*; Fig. 5, *D–F*, compare *lanes 1* and *2*). They were the translation products of residual endogenous microsomal mRNAs rather than glycosylated forms of mPRA1 mutants, because they were produced even in the absence of the mPRA1 transcript (Fig. 5*C*, compare *lanes 6* and *7*; data not shown).

The topography of these mPRA1 mutants was also examined *in vivo*. In this case, the proteins were expressed in BHK cells, and the protein synthesis was monitored by pulse-chase labeling experiments with [^{35}S]methionine as the radioactive label. Cell lysates were immunoprecipitated by the goat antiserum specific for mPRA1, followed by SDS-PAGE and autoradiography (Fig. 5*G*). Immediately after a 5-min pulse labeling (0-min chase), the newly synthesized mPRA1 was seen as a single labeled product of 21 kDa. The mPRA1:G15N, mPRA1:G61S, and mPRA1:L115N mutants were identical to the wild-type mPRA1 in terms of electrophoresis mobility. The mPRA1-NLS mutant migrated slightly slower, reflecting the added *N*-linked glycosylation motif (NLS) at the C terminus. After a 30-min chase in a medium lacking [^{35}S]methionine, none of the mutants showed mobility shift (Fig. 5*G*), suggesting that none of the mutants were glycosylated. Consistent with this observation, treatment of the immunoprecipitates with Endo H and Endo F did not have any effect on the electrophoresis mobility of mPRA1 and the mutants (data not shown). Although the location of a given *N*-linked glycosylation site, *e.g.* the distance from the lipid bilayer, could affect the efficiency of glycosylation, the facts that none of the mutants contained any glycosylation both *in vitro* and *in vivo* and that mPRA1 contained four TM segments (see above) strongly suggested that the N, L, and C domains were all located on the cytoplasmic side of the membrane.

To further establish the topography of mPRA1, we inserted the N-terminal 52-residue fragment of the TAIL domain (TAIL*), which contained three glycosylation sites, between TM1 and TM2 as well as between TM3 and TM4 of mPRA1 (Fig. 6*A*). The resulting chimeras mPRA (TM1-TAIL*-TM2) and mPRA(TM3-TAIL*-TM4) were translated *in vitro* in the absence and

NIH-PA Author Manuscript

NIH-PA Author Manuscript

NIH-PA Author Manuscript

presence of microsomes. The mPRA-TM1-TAIL*-TM2 was about 90% glycosylated when translated in the presence of microsomes (Fig. 6*B*, *lane 2*, *arrowhead*). The glycosylated protein was essentially insoluble in the carbonate buffer (Fig. 6*B*, *lanes 4–6*). Proteinase K digestion yielded two proteolytic products (Fig. 6*B*, *lane 7*), which were both sensitive to Endo H treatment (Fig. 6*B*, compare *lanes 10* and *11*). The molecular mass of the larger product correlated to that of the mPRA(TM1-TAIL*-TM2) fragment lacking the N- and C-terminal domains, whereas the smaller product correlated to the fragment lacking not only the N- and C-terminal domains but also the L and HD2 domains. The data confirmed that HD1 contained two authentic TM segments with TM1 functioning as a signal sequence that translocates the TAIL* sequence into the lumen and TM2 functioning as a stop-transfer sequence that halts the translocation and keeps the downstream sequence in the cytoplasm. In contrast to mPRA95-TAIL, which contained only the TM1 segment and was poorly glycosylated and soluble in the carbonate buffer, mPRA(TM1-TAIL*-TM2) became mostly glycosylated and insoluble in the carbonate buffer, indicating that the TM2 segment increased the translocation and integration efficiency to the extent that could not be reached by TM1 alone.

Similar results were obtained for mPRA(TM3-TAIL*-TM4). About 50% of the proteins synthesized in the presence of microsomes were glycosylated, and the glycosylated proteins were insoluble in the carbonate buffer (Fig. 6*C*). The signal of the full-length translation product (Fig. 6*C*, *arrow*) was somewhat compromised by the presence of two prominent premature termination products. As a result, it took longer exposure time of the gel to detect the proteinase K-digested products. The prominent proteolytic product correlated to the mPRA(TM3-TAIL*-TM4) fragment lacking the N- and C-terminal domains (Fig. 6*C*, *lane 7*). After Endo H treatment, the signal of the proteolytic product became too weak to be detected (data not shown). The data suggested that HD2, like HD1, also contained two TM segments, with one (TM3) functioning as a signal sequence and the other (TM4) as a stop-transfer sequence. Once again, a downstream TM segment facilitated the translocation and integration process that the upstream TM segment by itself was unable to accomplish.

DISCUSSION

Topography

We have demonstrated experimentally that mPRA1 is an integral membrane protein with the following topography. The hydrophilic N-terminal domain (residues 1–78), the L domain (residues 113–131), and the C-terminal domain (residues 166–185) are in the cytoplasm. Each of the hydrophobic domains (HD1 (residues 79–112) and HD2 (residues 132–165)) spans the membrane bilayer as a pair of TM segments (TM1/TM2 and TM3/TM4, respectively). Our results have confirmed one of the theoretically predicted topologies (Fig. 1*D*).

The cytoplasmic N and L domains of mPRA1 contain three Arg and Lys residues within 20 residues of HD1 and HD2. This mPRA1 topography is consistent with the “positive inside” rule, which was originally derived from statistical analyses of prokaryotic membrane proteins and was later shown to be applicable to eukaryotic membrane proteins as well (9,10,22). Unlike some polytopic membrane proteins, however, mPRA1 does not have any hydrophilic domains located in the luminal side of the membrane. This topography may result in somewhat less stable association of PRA1 with the membrane (4). In agreement with this notion, only about 50% of *in vitro* synthesized mPRA1 and mPRA1-TAIL fusion proteins (exclude mPRA95-TAIL) are associated with the membrane after sodium carbonate extraction, although more than 90% of the proteins are targeted to the membrane as judged by their resistance to extractions with 0.5 M KOAc or 25 mM EDTA (data not shown). When a hydrophilic segment is added to the luminal side of mPRA1, the resulting chimeric protein, mPRA(TM1-TAIL*-TM2) or mPRA(TM3-TAIL*-TM4), becomes much more stably associated with the membrane *in vitro*.

NIH-PA Author Manuscript

NIH-PA Author Manuscript

NIH-PA Author Manuscript

Topogenesis

The data provide insights into the topogenesis of mPRA1 at the ER membrane, which sheds light on the mechanism of translocation and integration of polytopic membrane proteins into the membrane in general. Because the mPRA1 contains four TM segments, according to the classic sequential insertion model (23), the odd-numbered TM sequence should function as a signal sequence to target the nascent chain-ribosome complex to the ER membrane and to translocate the downstream sequence across the membrane. The even-numbered TM sequence should function as a stop-transfer sequence to halt the translocation and to initiate integration of TM sequences into the membrane. Some of our data support this model. For example, the TM1 segment indeed functions as a signal sequence that targets the nascent mPRA1 chain to the ER membrane in an SRP-dependent reaction and translocates downstream sequences (if provided) across the membrane. Other data of this study, however, do not strictly follow the sequential insertion model. For example, the TM3 segment alone cannot translocate downstream sequences across the membrane. However, when TM3 is paired with another TM segment (TM4), which can be as far as 52 residues downstream, the TM3 segment then functions as a signal sequence to translocate the 52 residues across the membrane. Even for TM1, which can function independently of TM2, the addition of TM2 significantly increases both translocation and integration efficiency. Therefore, TM1/TM2 and TM3/TM4 actually function as two pairs of cooperative TM segments that translocate and integrate mPRA1 efficiently into the ER membrane.

The finding that it takes two mPRA1 TM segments to integrate into the membrane has precedents in the topogenesis of other polytopic membrane proteins such as the *Neurospora* H^+-ATPase and the human P-glycoprotein (19,20). In the case of P-glycoprotein, although the first or the second TM segment can translocate the C-terminal sequence across the membrane, neither segment alone can integrate the protein into the bi-layer. The integration requires both TM segments to work cooperatively. In *Neurospora* H^+-ATPase, neither the first nor the second TM segment alone is sufficient to integrate a fusion protein into the ER membrane. When both TM segments are present, the fusion protein can be integrated effectively into the membrane. Unlike the TM segments of mPRA1 that are still functional when separated by as many as 52 residues, however, TM1 and TM2 of *Neurospora* H^+-ATPase are not able to translocate and integrate a fusion protein into the membrane when separated by a similar number of residues.

Both translocation and integration occur at the ER translocon (5). If two TM segments cooperate in these processes, one possibility is that both TM segments are detected at the translocon in the ER membrane. For two TM segments that are 52 residues apart (*e.g.* mPRA (TM1-TAIL*-TM2)), this would require the translocation initiated by the first TM segment to take place to move the second TM segment to the translocon. In the case mPRA(TM3-TAIL*-TM4), however, TM3 by itself cannot initiate translocation, making it difficult to bring the downstream TM4 to the translocon. This can be reconciled if the ribosome can detect the TM4 segment right after it is synthesized and send a signal to the translocon to allow the translocation of TM3 to take place. In this regard, a recent study has suggested that the ribosome can indeed detect a TM segment and regulate the translocon gating function (18).

What type of TM segment can act independently as a topogenic sequence? Hydrophobicity is an important factor for a segment to be recognized as a signal or stop-transfer sequence by the translocation machinery (24–26). The TM3 segment alone cannot function as either a signal sequence or a stop-transfer sequence, possibly due to its relatively low hydrophobicity (Fig. 1*B*). The fact that the more hydrophobic TM1 functions both as a signal and as a stop-transfer sequence supports this view. It is also known that sequence context of a hydrophobic segment can influence its topogenic function (27). We show here that TM4 can function as a stop-transfer sequence in 111p-TM4, yet it cannot function as a signal sequence in mPRA165-TAIL. For TM1, it functions as an almost perfect stop-transfer sequence in 111p-TM1, but it is a rather

NIH-PA Author Manuscript

NIH-PA Author Manuscript

NIH-PA Author Manuscript

weak signal sequence in mPRA95-TAIL and translocates only 10% of the TAIL sequences across the membrane *in vitro*. Interestingly these 10% of proteins cannot integrate into the bilayer. Instead they appear to be trapped in the translocon (hence extractable by the carbonate buffer), possibly due to the interaction of the TM segment with the translocon proteins (12).

Determination of Membrane Topography in Vitro and in Vivo

This study has used both *in vitro* and *in vivo* systems to determine the membrane topography of mPRA1. The advantage of using the *in vitro* system is that it is relatively easy to map the membrane topography using a variety of reporter groups or treatments (28). *In vitro* reconstitution of the *in vivo* targeting, translocation, or integration process allows one to identify the components required for topogenesis of secretory and membrane proteins (29–31). For example, we show here with the *in vitro* system that the SRP is required for the membrane targeting of mPRA1. The *in vivo* system, on the other hand, is closer to the physiological condition and hence complementary to the *in vitro* system. In this study, the *in vitro* and *in vivo* data are consistent and thus validate the conclusions on the mPRA1 topography. We notice some quantitative differences between the two systems. For example, only about 10% of the targeted mPRA95-TAIL molecules have their TAIL sequences translocated across the membrane, and a negligible amount of this protein is integrated into the membrane *in vitro*. Yet when expressed *in vivo*, the same protein is fully integrated with the TAIL sequence translocated, indicating that the translocation and integration processes are more efficient *in vivo* than *in vitro*. It is possible that some auxiliary factors for the translocation and integration processes are limiting in the *in vitro* system. Interestingly, adding another TM segment to form a functional pair of TM segments can reduce the dependence on these auxiliary factors *in vitro*.

Function

Although the mPRA1 topography gives us a better understanding of mPRA1 function, it has not yet been firmly established. The Golgi localization and ability of mPRA to interact with Rab proteins suggests that it may play a role in Golgi membrane trafficking. Overexpression of mPRA1 and its truncation mutants does not have a significant effect on the anterograde transport of a marker protein (the Sindbis virus E2 protein) through the Golgi complex (1). Although these negative results do not necessarily rule out the involvement of mPRA1 in the anterograde transport, an alternative possibility is that mPRA1 may function in the retrograde transport mediated by the Golgi-associated Rab6 protein (32). Because the PRA protein interacts with all Rabs tested so far in the yeast two-hybrid system (1–3), it is also likely to be a generic factor for the initial recruitment of newly synthesized Rab molecules to the membrane. A recent biochemical study suggests that PRA1 can counteract the action of GDP-dissociation inhibitor and regulate the membrane association of Rab proteins (4). These protein interactions should occur on the cytoplasmic side of the membrane. The mPRA1 membrane topography established in this study indicates that the bulk of its polypeptide indeed faces the cytoplasm and may interact with cytoplasmic factors.

References

1. Liang Z, Li G. Biochem Biophy Res Commun 2000;275:509–516.
2. Martincic I, Peralta ME, Ngsee JK. J Biol Chem 1997;272:26991–26998. [PubMed: 9341137]
3. Bucci C, Chiariello M, Lattero D, Maiorano M, Bruni CB. Biochem Biophys Res Commun 1999;258:657–662. [PubMed: 10329441]
4. Hutt DM, Da-Silva LF, Chang LH, Prosser DC, Ngsee JK. J Biol Chem 2000;275:18511–18519. [PubMed: 10751420]
5. Johnson AE, van Waes MA. Annu Rev Cell Dev Biol 1999;15:799–842. [PubMed: 10611978]
6. Palade G. Science 1975;189:347–358. [PubMed: 1096303]

NIH-PA Author Manuscript

NIH-PA Author Manuscript

NIH-PA Author Manuscript

7. Kyte J, Doolittle RF. J Mol Biol 1982;157:105–132. [PubMed: 7108955]
8. Denzer AJ, Nabholz CE, Spiess M. EMBO J 1995;14:6311–6317. [PubMed: 8557050]
9. Hartmann E, Rapoport TA, Lodish HF. Proc Natl Acad Sci U S A 1989;86:5786–5790. [PubMed: 2762295]
10. von Heijne G. Annu Rev Biophys Biomol Struct 1994;23:167–192. [PubMed: 7919780]
11. Falcone D, Andrews DW. Mol Cell Biol 1991;11:2656–2664. [PubMed: 2017171]
12. Do H, Falcone D, Lin J, Andrews DW, Johnson AE. Cell 1996;85:369–378. [PubMed: 8616892]
13. Gurevich VV, Pokrovskaya ID, Obukhova TA, Zozulya SA. Anal Biochem 1991;195:207–213. [PubMed: 1750668]
14. Erickson AH, Blobel G. Methods Enzymol 1983;96:38–50. [PubMed: 6656637]
15. Walter P, Blobel G. Methods Enzymol 1983;96:682–691. [PubMed: 6197610]
16. Anderson DJ, Blobel G. Methods Enzymol 1983;96:111–120. [PubMed: 6361451]
17. Bordier C. J Biol Chem 1981;256:1604–1607. [PubMed: 6257680]
18. Liao S, Lin J, Do H, Johnson AE. Cell 1997;90:31–41. [PubMed: 9230300]
19. Lin J, Addison R. J Biol Chem 1995;270:6935–6941. [PubMed: 7896843]
20. Skach WR, Lingappa VR. J Biol Chem 1993;268:23552–23561. [PubMed: 7901209]
21. Wilkinson BM, Critchley AJ, Stirling CJ. J Biol Chem 1996;271:25590–25597. [PubMed: 8810333]
22. Gafvelin G, Sakaguchi M, Andersson H, von Heijne G. J Biol Chem 1997;272:6119–6127. [PubMed: 9045622]
23. Blobel G. Proc Natl Acad Sci U S A 1980;77:4160–4164. [PubMed: 6254013]
24. Chen H, Kendall DA. J Biol Chem 1995;270:14115–14122. [PubMed: 7775472]
25. Kuroiwa T, Sakaguchi M, Mihara K, Omura T. J Biol Chem 1991;266:9251–9255. [PubMed: 2026623]
26. Wahlberg JM, Spiess M. J Cell Biol 1997;137:555–562. [PubMed: 9151664]
27. Goder V, Bieri C, Spiess M. J Cell Biol 1999;147:257–266. [PubMed: 10525533]
28. Wessels HP, Beltzer JP, Spiess M. Methods Cell Biol 1991;34:287–302. [PubMed: 1943805]
29. Gorlich D, Rapoport TA. Cell 1993;75:615–630. [PubMed: 8242738]
30. Hamman BH, Hendershot LM, Johnson AE. Cell 1999;92:747–758. [PubMed: 9529251]
31. Nicchitta CV, Blobel G. Cell 1993;73:989–998. [PubMed: 8500184]
32. Martinez O, Antony C, Pehau-Arnaudet G, Berger EG, Salamero J, Goud B. Proc Natl Acad Sci U S A 1997;94:1828–1833. [PubMed: 9050864]

NIH-PA Author Manuscript

NIH-PA Author Manuscript

NIH-PA Author Manuscript

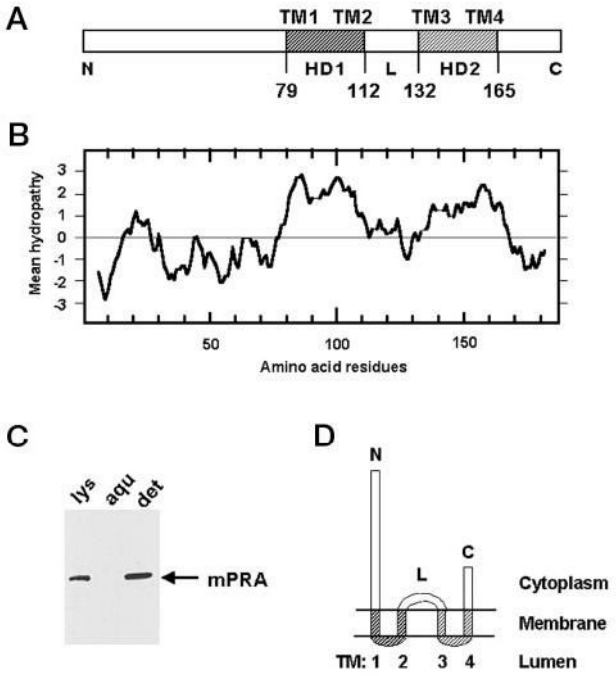

Fig. 1. Schematic structure, hydropathy plot, membrane association, and membrane topography model of mPRA1.

A, schematic structure of mPRA1. *HD1* and *HD2* represent the two internal hydrophobic domains interspersed between three hydrophilic domains: the N-terminal domain (*N*), the linker domain (*L*), and the C-terminal domain (*C*). The *numbers* indicate the positions of the residues that mark the start and the end of HD1 and HD2. Each HD is of sufficient length to contain two transmembrane (*TM*) segments: TM1 and TM2 in HD1, TM3 and TM4 in HD2. *B*, Kyte-Doolittle hydropathy plot, which reveals the two hydrophobic domains corresponding to HD1 and HD2. *C*, an immunoblot indicating that mPRA1 in the cell lysate (*lys*) completely partitions into the detergent (*det*) phase (*versus* the aqueous (aqu) phase) in the Triton X-114 partitioning experiment, as expected for an integral membrane protein. *D*, shown is a topography model of mPRA1. Four TM segments anchor the protein in the membrane with all hydrophilic domains located in the cytoplasm.

NIH-PA Author Manuscript

NIH-PA Author Manuscript

NIH-PA Author Manuscript

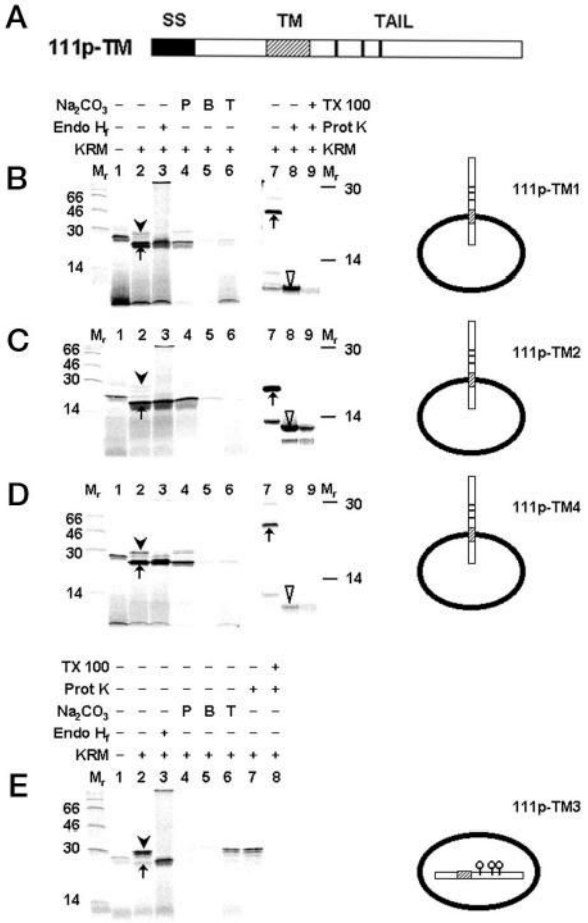

Fig. 2. Membrane topography of 111p-TM chimeric proteins.

A, shown is a schematic structure of the model membrane protein 111p. Its primary sequence was described previously (18). The 111p contains two topogenic sequences, including a cleavable N-terminal signal sequence (*SS*) and a transmembrane (*TM*) segment. The C-terminal tail (*TAIL*) of 111p contains three *N*-linked glycosylation sites (*vertical bars*). In the experiments, the TM segment of 111p is replaced by TM1 (residues 79–94), TM2 (residues 95–112), TM3 (residues 132–148), or TM4 (residues 149–165) of mPRA1. *B–E*, the mRNAs of 111p-TM1 (*B*), 111p-TM2 (*C*), 111p-TM4 (*D*), and 111p-TM3 (*E*) were translated in wheat germ extracts in the presence of [^{35}S]Met, SRP, and in the absence or the presence of microsomal membranes (− or +*KRM*). Aliquots of each sample were treated with Endo H (+*Endo H*), proteinase K (+*Prot K*), or carbonate buffer, pH11.5 (*Na_2CO_3*). The proteinase K treatment was done in the absence or the presence of Triton X-100 (− or +*TX 100*). Following carbonate treatment, the samples were separated into the top (*T*), the bottom (*B*), and the membrane pellet (*P*) fractions by centrifugation. All samples were quantified by using a PhosphorImager, following SDS-PAGE with a 14% (all lanes except *lanes 7–9*) or a 10–15% (*lanes 7–9*) acrylamide gel. *Arrows*, *arrowheads*, and *triangles* indicate signal sequence-cleaved, glycosylated, and proteolytic products, respectively. The molecular mass of the major proteolytic product in *lane 8* of *panels B–D* correlates to that of the N-terminal and TM sequences of 111p-TM. Molecular mass standards (lane M_r, in kilodaltons) are indicated on the left for *lanes 1–6* of *B–D* and all lanes of *E*. They are indicated on the *right* for *lanes 7–9* of *B–D*. The membrane topography of each 111p-TM chimera is schematically illustrated on the *right*, based on the results. The ovals represent the membranes of microsomal vesicles. The

three small circles attached to the TAIL of 111p-TM3 indicate the three *N*-linked oligosaccharide moieties.

NIH-PA Author Manuscript
NIH-PA Author Manuscript
NIH-PA Author Manuscript

NIH-PA Author Manuscript

NIH-PA Author Manuscript

NIH-PA Author Manuscript

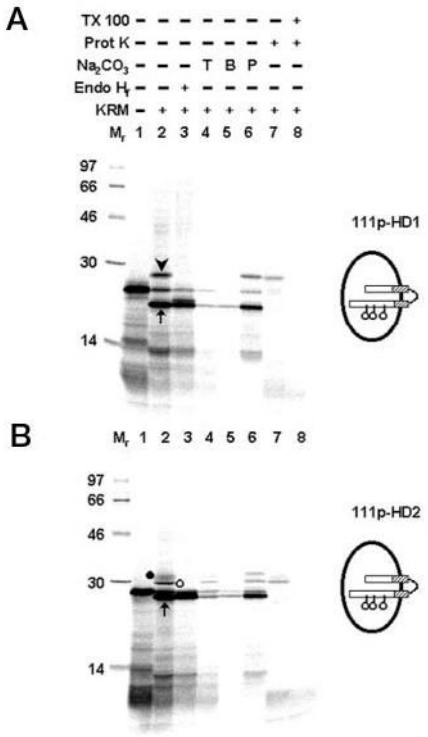

Fig. 3. Membrane topography of 111p-HD chimeric proteins.

The *in vitro* translation reactions and the various treatments are the same as those described in the Fig. 2 legend except that the mRNAs of 111p-HD1 (*A*) and 111p-HD2 (*B*) are the exogenously added templates for translation. Shown are autoradiographs of dried 10–15% acrylamide gels containing the translation products. The *open* and *closed circles* in *panel B* denote the glycosylated forms I and II of 111-HD2, respectively.

NIH-PA Author Manuscript

NIH-PA Author Manuscript

NIH-PA Author Manuscript

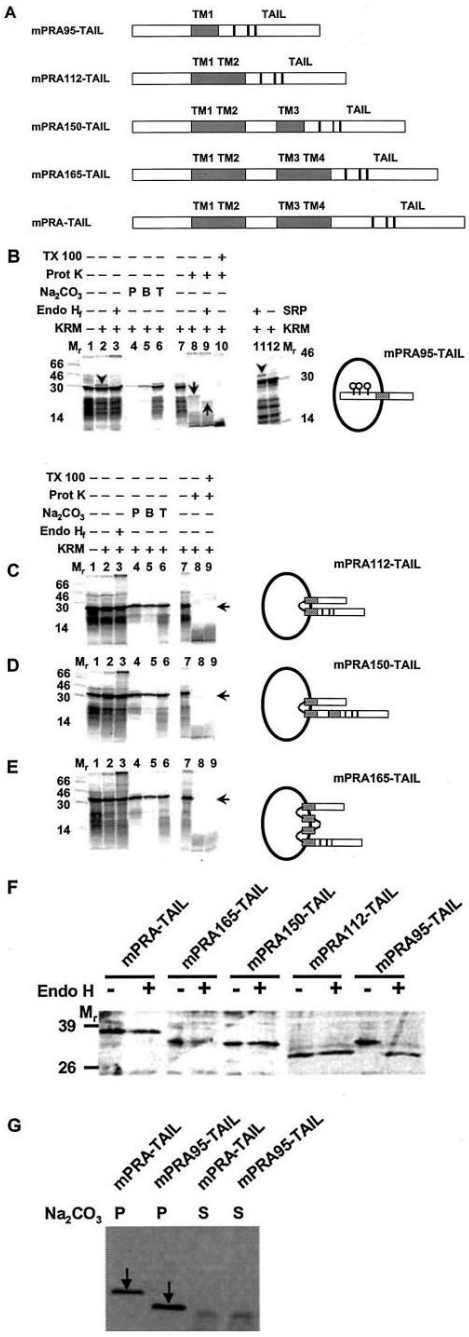

Fig. 4. Membrane topography of mPRA1-TAIL chimeric proteins.

A, the schematic structures of mPRA1-TAIL chimeras are depicted. Each chimera contains an N-terminal fragment of mPRA1 fused to the TAIL domain of 111p. The mPRA1 fragments terminate at the end of each putative TM segment, *e.g.* mPRA95-TAIL contains the N-terminal 95 residues of mPRA1, which terminates after TM1. The mPRA-TAIL protein contains the full-length mPRA1 fused to the TAIL domain. *B–E*, the experiments were done as described in the Fig. 2 legend, except for *lanes 11* and *12* of *panel B* where the mRNAs were translated in the absence or the presence of SRP (− or +*SRP*). All SDS-PAGE analyses were done using a 14% acrylamide gel except for *lanes 11* and *12* where a 10–15% gel was used. In *panel B*, *arrowheads* indicate glycosylated products whereas *downward* and *upward arrows* indicate

NIH-PA Author Manuscript

NIH-PA Author Manuscript

NIH-PA Author Manuscript

the untreated and Endo H-treated proteolytic products, respectively. The molecular mass of the Endo H-treated proteolytic product correlates to that of the mPRA95-TAIL fragment containing the protected TM1 and TAIL sequences. In *C–E*, the *arrows* indicate the translation products of corresponding mPRA-TAIL chimeras. Membrane topography of each mPRA-TAIL chimera is schematically illustrated on the *right*, based on the results. *F*, the mPRA-TAIL chimeras were expressed in BHK cells. Aliquots of the cell lysates were either treated or not treated with Endo H (− or +*Endo H*). The mPRA-TAIL chimeras were identified by immunoblot analysis using the goat antiserum monospecific for mPRA1. The results are shown with the molecular mass standards (in kilodaltons) indicated on the *left. G*, the mPRA95-TAIL and mPRA-TAIL were expressed in BHK cells. Post-nuclear membrane fractions were prepared from the cells and treated with the carbonate buffer (pH 11.5). The samples were then separated into soluble (*S*) and membrane pellet (*P*) fractions by centrifugation and subjected to the immunoblot analysis as described above in *F*. *Arrows* indicate the mPRA-TAIL and mPRA95-TAIL proteins in the membrane pellet fractions.

NIH-PA Author Manuscript

NIH-PA Author Manuscript

NIH-PA Author Manuscript

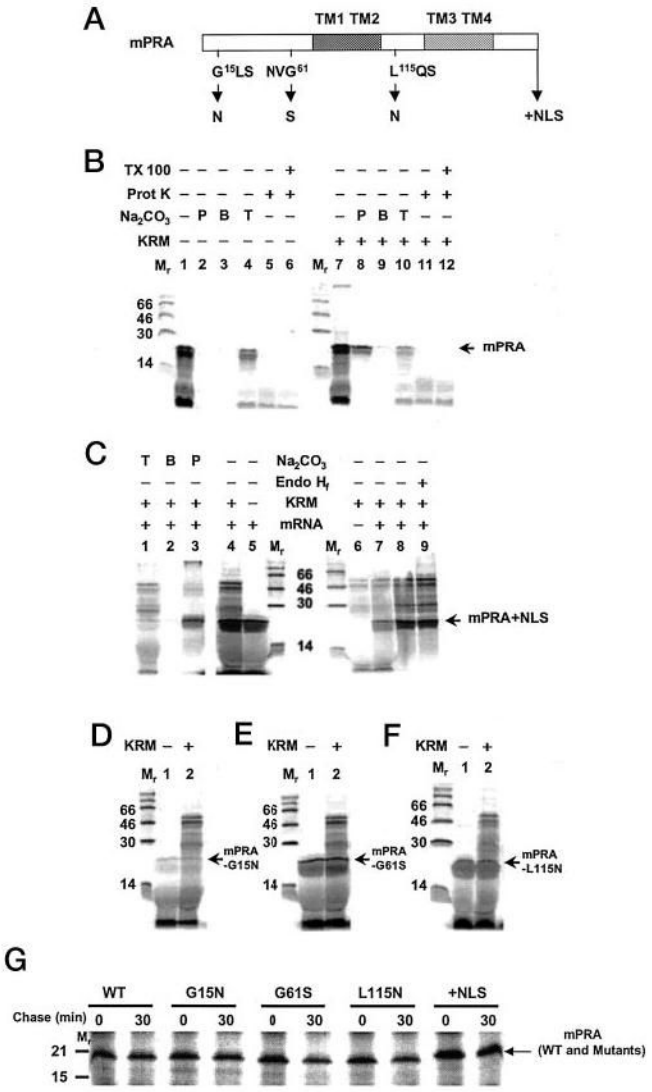

Fig. 5. Membrane topography of mPRA1 and mPRA1 mutants with glycosylation sites inserted in the hydrophilic sequences.

A, the primary structure of mPRA1 was depicted to show the locations of four putative TM segments and four engineered *N*-linked glycosylation sites (N*X*(S/T)). *Single-letter amino acid code* is used, with *superscript numbers* denoting the positions of mutated residues. The mutations are indicated by *arrows*. *+NLS* represents the three amino acid residues added to the C terminus. *B–F*, the experiments were done as described in the Fig. 2 legend, except that the mRNAs were translated in rabbit reticulocyte lysates. *Arrows* indicate the translation products of mPRA1 and the four mutants. *G*, the mPRA1 and the four mutants were expressed in BHK cells. The cells were pulse-labeled for 5 min with [^{35}S]Met and chased for 30 min as indicated, followed by immunoprecipitation with the goat antiserum for mPRA1, SDS-PAGE, and autoradiography as described under "Experimental Procedures." Molecular mass standards (in kilodaltons) are indicated on the left. The *arrow* on the *right* indicates the expressed mPRA1 and mutants.

NIH-PA Author Manuscript

NIH-PA Author Manuscript

NIH-PA Author Manuscript

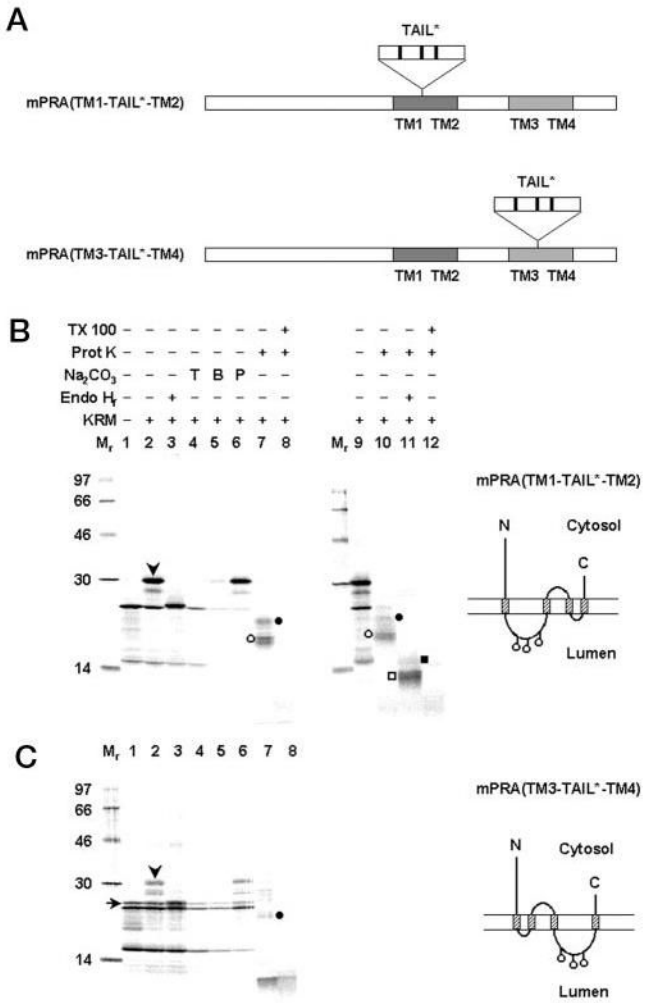

Fig. 6. Membrane topography of mPRA1 chimeras with glycosylation sites inserted in the hydrophobic sequences (*HD1* and *HD2*).

A, schematic structures of the mPRA1 chimeras are depicted to show the four TM segments and the location of the inserted TAIL* sequence that contains three *N*-linked glycosylation sites. *B* and *C*, shown are phosphorimages of dried 10–15% acrylamide gels containing the translation products. The *in vitro* translation reactions and the various treatments are the same as those described in the Fig. 2 legend. The *arrowheads* indicate the glycosylated products whereas *open* and *closed circles* indicate proteolytic products. In *B*, the *open* and *closed squares* indicate the proteolytic products after Endo H treatment. In *C*, the *arrow* indicates the full-length translation product of mPRA(TM3-TAIL*-TM4).